ChemPubSoc Europe

DOI: 10.1002/ejoc.201600806

European Journal of Organic Chemistry

Full Paper

Two-Photon Absorption

Synthesis, Fluorescence, and Two-Photon Absorption Properties of Push–Pull 5-Arylthieno[3,2-*b*]thiophene Derivatives

M. Manuela M. Raposo,*[a] Cyril Herbivo,[a] Vincent Hugues,[b] Guillaume Clermont,[b] M. Cidália R. Castro,[a] Alain Comel,[c] and Mireille Blanchard-Desce*[b]

Abstract: Three series of novel push–pull 5-arylthieno[3,2-*b*]-thiophene derivatives functionalized with potent electron-withdrawing terminal moieties have been synthesized in moderate to excellent yields by Suzuki coupling followed by Knoevenagel condensation. These novel chromophores show intense absorption in the near-UV region through to the orange visible region, related to a strong intramolecular charge-transfer transition. By combining a strong donor and acceptor, large fluorescence quantum yields were achieved as well as large two-photon absorption responses. Interestingly, due to the improved rigidity and electronic delocalization provided by the thienothiophene moiety (as compared with the bithiophene unit), higher one- and two-photon brightness values have been achieved. As a result, several new fluorescent dyes showing enhanced brightness and tunable fluorescence (ranging from the blue to the NIR region) have been obtained that have potential for bioimaging applications.

Introduction

Organic materials displaying strong two-photon absorption (TPA)[1–3] have attracted great interest due to their potential applications in photonics and optoelectronics, including 3D optical data storage,[4] 3D microfabrication,[5] optical limitation,[6] and two-photon microscopy (TPM).[7] For microscopic imaging, in particular for in vivo imaging, the two-photon excitation process presents several advantages as it provides intrinsic 3D resolution and improved in-depth tissue penetration.[7] Furthermore, the combination of two-photon absorption with efficient singlet-oxygen generation provides potential for the further development of photodynamic cancer therapy (PDT) methods.[8] Although considerable effort has been devoted to developing TPA dyes, the fluorescent quantum yields are often lower than desired, and photobleaching can be a shortcoming for real applications. In addition to strong two-photon absorption, high two-photon excited fluorescence (TPEF) cross-sections (i.e., two-photon brightness), good photostability, and appreciable solubility are also required for practical applications.[1]

Strong two-photon absorption is often correlated with significant intermolecular charge transfer (ICT) processes. Hence, a standard strategy for the design of molecules with large TPA cross-sections is based on connecting electron-rich donor entities (D) with electron-deficient acceptors (A) through π-electron conjugated bridges within conjugated structures of various topology. Different factors influence the TPA, including the conjugation length and its modulation, the molecular planarity, the dimensionality of the charge-transfer network, and the donating and withdrawing abilities of the electron-donor and -acceptor moieties. Different structural motifs have been employed in an attempt to optimize the TPA properties, including dipolar, quadrupolar, and octupolar structures in which ICT plays a major role, as well as conjugated branched or dendritic structures and macrocycles.[1–9] Although significant advances in the design of these materials have been made in recent years, there is still a need for improvement, in particular when strong TPA responses in the biological spectral window have to be combined with high fluorescence quantum yield, tunable fluorescence (in particular towards red- and NIR-emitting fluorophores), and photostability for imaging purposes. With this perspective, a promising approach is the replacement of aromatic systems with more easily delocalizable π-rich or π-deficient heteroaromatics, which has been shown to result in an increased ICT as well as an enhanced TPA, while preserving in many cases the chemical and photochemical stability of these systems. Moreover, modification of the structure by the incorporation of heterocycles into more complex π-conjugated systems allows the fine-tuning of the electronic and optical properties and often results in strong fluorescence emission, which is an essential prerequisite for certain TPA-based applications.[10] In this context, fused thienothiophene (TT) heterocyclic systems are expected to exhibit interesting TPA proper-

[a] *Center of Chemistry, University of Minho, Campus of Gualtar, 4710-057 Braga, Portugal*
E-mail: mfox@quimica.uminho.pt
http://www.cq.uminho.pt/
[b] *Univ. Bordeaux, Institut des Sciences Moléculaires (UMR 5255 CNRS), 33405 Talence, France*
E-mail: mireille.blanchard-desce@u-bordeaux.fr
http://www.ism.u-bordeaux1.fr/spip.php?article1996&lang=fr
[c] *Université de Lorraine, Institut Jean Barriol, Laboratoire de Chimie et Physique – Analyse Multi-échelles des Milieux Complexes, 57048 Metz Cedex, France*

Supporting information for this article is available on the WWW under http://dx.doi.org/10.1002/ejoc.201600806.

ties due to their lower resonance energy per electron when compared with thiophene as well as greater electronic relay and planarity compared with the bithiophene counterpart. These features would also allow an increase in the conjugation between the donor (D) and acceptor (A), which typically results in increased NLO responses and improved thermal stability as well as a good transparency/nonlinearity trade-off.[11,12]

In the last 30 years, several investigators have reported the synthesis and characterization of functionalized thienothiophene (TT) derivatives having in mind primarily their application in materials and medicinal chemistry due to their interesting optoelectronic properties and high thermal and chemical stabilities as well as wide range of biological activities.[13] In materials chemistry these derivatives have found application in several areas, for example, nonlinear optics (NLO),[11] dye-sensitized solar cells (DSSCs),[14] liquid crystals,[15] organic light-emitting diodes (OLEDs),[16] organic semiconductors, field-effect transistors, and conducting polymers.[17] Despite their diverse and interesting applications, the synthesis and reactivity studies of thienothiophene derivatives are less developed compared with other thiophene derivatives, probably due to synthetic difficulties.[13]

In recent years we have been engaged in the synthesis of novel formyl-heterocyclic systems [bithiophenes, oligothiophenes, aryl(bi)thiophenes, (thienyl)pyrroles][18] through different synthetic methodologies. These heterocyclic carbaldehydes proved to be versatile precursors for the synthesis of dicyanovinyl and thiobarbituric acid derivatives with interesting second-order nonlinear optical properties.[18a,18b,18f,19] We have also reported the synthesis, photophysical, and TPA properties of a series of push–pull arylbithiophene chromophores bearing alkoxy and dialkylamino electron-donating (D) groups and formyl, dicyanovinyl, and 1,3-diethyl-2-thioxodihydropyrimidine-4,6-dione electron-withdrawing (A) end groups.[18e,20] In contrast to the corresponding push–pull polyenes,[21] these chromophores bearing a phenylbithienyl conjugated path exhibit a significant increase in fluorescence. Additionally, some of these chromophores combine very large one- and two-photon brightness as well as sizeable emission in the red/NIR region, and are therefore promising biphotonic fluorescent probes for bioimaging.[20b]

Moreover, despite the large number of donor–acceptor heterocyclic systems showing TPA properties reported in the literature, the concept of linking 4-alkoxy and 4-(dialkylamino) groups with an arylthieno[3,2-*b*]thiophene bridge functionalized with a strong dicyanovinyl or 1,3-diethyl-2-thioxodihydropyrimidine-4,6-dione acceptor group has not, to the best of our knowledge, been previously communicated in the literature. Additionally, few examples of thienothiophenes have been investigated for nonlinear optical applications and only as NLO-phores for second-harmonic generation.[11]

We were therefore motivated to extend our previous studies to explore the potential of three new series of push–pull arylthienothiophene heterocyclic systems **8**–**10**. Consequently, we report herein the synthesis and a detailed study of the fluorescence and TPA properties of arylthienothiophene derivatives **8**–**10** bearing various electron-donating (OR, NR_2) and electron-withdrawing (formyl, dicyanovinyl, and barbiturate) end groups (EWG) and an arylthieno[3,2-*b*]thiophene conjugated bridge.

Results and Discussion

Synthesis

For the reasons described above, we decided to focus on the synthesis and characterization of the optical and thermal properties of *p*-alkoxy- and *p*-(dialkylamino)-substituted 5-arylthieno[3,2-*b*]thiophene-2-carbaldehydes **8** and the corresponding dicyanovinyl (**9**) and barbiturate (**10**) derivatives easily obtained through Knoevenagel condensation reactions.

Surprisingly, only a few reports have described the synthesis of 5-arylthieno[3,2-*b*]thiophene derivatives. One recent report[22] described the preparation of a 2-(*p*-alkoxyphenyl)-thieno[3,2-*b*]thiophene derivative. The synthetic method reported in this paper is original, based on a domino thiolation/cyclization reaction that can also be applied to the synthesis of benzo[*b*]thiophenes and thieno[3,2-*b*]thiophenes. Previously, 2-arylthieno[3,2-*b*]thiophenes functionalized with acceptor groups (NO_2, CN, CO_2Me, SO_2Me) at the *para* position of the phenyl ring have been prepared by a palladium-catalyzed arylation of thieno[3,2-*b*]thiophene or intramolecular cyclization of 2,3-disubstituted thiophenes.[23] On the other hand, the synthesis of 5-[(diphenylamino)phenyl]-substituted thieno[3,2-*b*]thiophene-2-carbaldehydes or -carboxylates is better documented.[14] These compounds are generally the starting points of structurally more complex organic sensitizers designed for application in DSSCs. Two different synthetic strategies have generally been reported, both involving classical coupling reactions under mainly Suzuki, Suzuki–Miyaura, and Stille conditions.[14] An a priori prepared or commercially available (thieno[3,2-*b*]thiophen-2-yl)boronic acid or (thieno[3,2-*b*]thiophen-2-yl)stannane can react with a suitable aryl bromide, or an arylstannane can be coupled with a 5-substituted or unsubstituted 2-bromo- (or 2-iodo-) thieno[3,2-*b*]thiophene. The 5-[(diphenylamino)phenyl]thieno[3,2-*b*]thiophene can be further functionalized[14g] or deprotected[14c,14h] depending on the thienothiophene derivative used.

Synthesis of Aldehydes 8 through Suzuki Coupling

To prepare carbaldehydes **8**, we first synthesized the thieno-[3,2-*b*]thiophene-2-carbaldehyde precursor **5** by the combination of two synthetic methodologies described earlier by Fuller[24] and Prugh et al.[25] Thus, methyl thieno[3,2-*b*]thiophene-2-carboxylate (**3**) was synthesized by the method of Fuller et al., followed by reduction of the ester in **3** with lithium aluminium hydride to give alcohol **4**, which was re-oxidized with pyridinium chlorochromate (PCC) to thieno[3,2-*b*]thiophene-2-carbaldehyde (**5**).[25] The reaction of **5** with bromine in chloroform at 0 °C to room temperature gave 5-bromothieno-

[3,2-*b*]thiophene-2-carbaldehyde (**6**) as a pale-yellow solid in 88 % yield (Scheme 1). Two different methods for the synthesis of compound **6** have been reported recently, namely the lithiation of 2,5-dibromothieno[3,2-*b*]thiophene followed by reaction with DMF[14b] or the formylation of thieno[3,2-*b*]thiophene followed by bromination with *N*-bromosuccinimide (NBS).[26] However, in both cases, the characterization of compound **6** was incomplete.

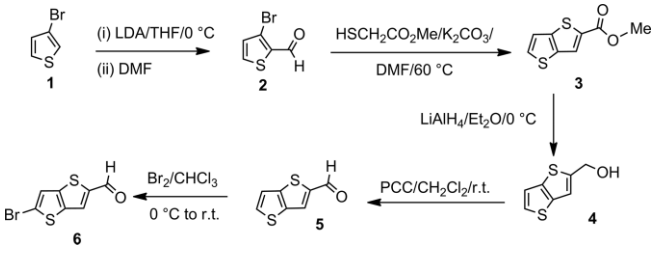

Scheme 1. Synthesis of precursor **6**.

Aldehydes **8** were prepared by Suzuki reaction of commercially available arylboronic acids **7a**–**e** with 5-bromothieno-[3,2-*b*]thiophene-2-carbaldehyde (**6**). The Suzuki cross-coupling reactions were performed under nitrogen using two different sets of reaction conditions: Method A using 1,2-dimethoxyethane (DME), $[Pd(PPh_3)_4]$ (6 %), Na_2CO_3, and H_2O at 80 °C;[18e,18f] and Method B using toluene, $[Pd(PPh_3)_4]$ (10 %), K_2CO_3, H_2O, and EtOH at reflux[27] (Scheme 2). In general, the formyl derivatives **8** were obtained in better yields (72–84 %) and in shorter reaction times by Method B (Table 1).

Synthesis of Dicyanovinyl (9) and Thiobarbituric Acid (10) Derivatives of Thieno[3,2-*b*]thiophene by the Knoevenagel Condensation Recations

Knoevenagel condensation of carbaldehydes **8** with malononitrile in dichloromethane at room temperature or with thiobarbituric acid in acetonitrile at reflux in the presence of a catalytic amount of piperidine gave dicyanovinyl derivatives **9** (Table 2, 49–81 % yields) and thiobarbituric acid derivatives **10** (Table 3, 42–82 % yields; Scheme 2), respectively.

Table 2. Yields, ^1H NMR, IR, and T_d data of the dicyanovinyl-arylthienothiophene derivatives **9**.

Aldehyde	R	Dicyanovinyl derivative	Yield [%]	δ_H [ppm][a]	$\tilde{\nu}$ [cm^{-1}][b]	T_d [°C][c]
8a	H	**9a**	54	8.76	2216	366
8b	MeO	**9b**	49	8.72	2219	390
8c	EtO	**9c**	74	8.71	2221	391
8d	NEt_2	**9d**	81	8.63[d]	2214	412

[a] Chemical shift of the *CH*=$(CN)_2$ proton of dicyanovinyl-arylthienothiophenes **9** (300 MHz, $[D_6]$DMSO). [b] All IR spectra were recorded in Nujol. [c] Decomposition temperature (T_d) measured at a heating rate of 20 °C min^{-1} under nitrogen, determined by thermogravimetric analysis (TGA). [d] Chemical shift of the *CH*=$(CN)_2$ proton of dicyanovinyl-arylthienothiophenes **9** (400 MHz, $[D_6]$DMSO).

The structures of the novel TT derivatives **8**–**10** were confirmed by their analytical and spectroscopic data. The most characteristic signals in the ^1H NMR spectra of aldehydes **8** are those corresponding to the *CH*O protons at $\delta \approx 9.90$–9.97 ppm. A singlet at $\delta \approx 8.63$–8.76 or 8.67–8.75 ppm can also be observed for the dicyanovinyl derivatives **9a**–**d** and the thio-

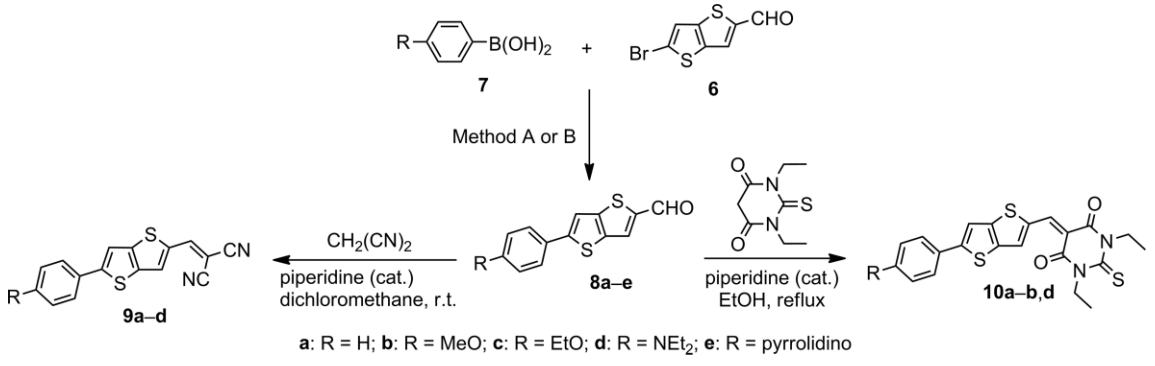

Scheme 2. Synthesis of aldehydes **8** by Suzuki coupling and subsequent synthesis of dicyanovinyl (**9**) and thiobarbituric acid (**10**) derivatives of thienothiophene by Knoevenagel condensation of the corresponding aldehyde precursors **8** with malononitrile or thiobarbituric acid, respectively.

Table 1. Synthesis of aldehydes **8a**–**e**.

	R	Method A[a]		Method B[b]		δ_H	$\tilde{\nu}$
		Reaction time [h]	Yield [%]	Reaction time [h]	Yield [%]	[ppm][c]	[cm^{-1}][d]
8a	H	24	35	1	80	9.97	1662
8b	MeO	4	50	1	72	9.94	1660
8c	EtO	4	85	1	79	9.94	1650
8d	NEt_2	4	36	2	84	9.91	1655
8e	pyrrolidino	4	30	2	70	9.90	1657

[a] Method A: DME, $[Pd(PPh_3)_4]$ (6 %), Na_2CO_3, H_2O, 80 °C. [b] Method B: toluene, $[Pd(PPh_3)_4]$ (10 %), K_2CO_3, H_2O, EtOH, reflux. [c] Chemical shift of the CHO proton of the arylthienothiophene-2-carbaldehydes **8** (300 MHz, $CDCl_3$). [d] All IR spectra were recorded in Nujol.

Table 3. Yields, ^{1}H NMR, IR, and T_d data of thiobarbituric acid thienothiophene derivatives **10**.

Aldehyde	R	Thiobarbituric acid derivative	Yield [%]	δ_H [ppm][a]	$\tilde{\nu}$ [cm^{-1}][b]	T_d [°C][c]
8a	H	**10a**	42	8.75	1682, 1654	333
8b	MeO	**10b**	74	8.74	1682, 1653	335
8d	NEt_2	**10d**	82	8.67[d]	1681, 1655	253

[a] Chemical shift of the C=C*H* proton of the thiobarbituric acid derivatives of arylthienothiophene **10** (400 MHz, [D$_6$]DMSO). [b] All IR spectra were recorded in Nujol. [c] Decomposition temperature (T_d) measured at a heating rate of 20 °C min^{-1} under nitrogen, determined by thermogravimetric analysis (TGA). [d] Chemical shift of the C=C*H* proton of the thiobarbituric acid derivatives of arylthienothiophene **10** (300 MHz, $CDCl_3$).

barbituric acid derivatives **10a**,**b**,**d**, respectively, which correspond to the vinylic proton of the ethylenic bridge (C=C*H*) linked to the dicyanovinyl or thiobarbituric acid acceptor moieties (Tables 1–3). Analysis of the ^{1}H NMR spectra of the push–pull systems **8**–**10** showed that the the C*H*O signal in compounds **8b**–**d** as well as the signal of the ethylene bridge (C=C*H*) linked to the acceptor moieties in derivatives **9b**–**d** and **10b**,**d** are shifted upfield relative to those of the corresponding unsubstituted derivatives **8a**, **9a**, and **10a**, due to the stronger mesomeric donor effect of the alkoxy and dialkylamino groups substituted at the *para* position of the aryl rings linked to the TT spacer. Moreover, a gradual slight upfield shift is observed with increasing donor strength.

IR spectroscopy was also used to identify the typical absorption bands of the carbonyl group in aldehydes **8** (1650–1662 cm^{-1}), the carbonyl (1653–1655 cm^{-1}) and thiocarbonyl groups (1681–1682 cm^{-1}) in thiobarbituric compounds **10**, and the nitrile groups in dicyanovinyl derivatives **9** (2214–2221 cm^{-1}).

Thermal Stability Studies

It is well known that good thermal stability is critical for the practical application of optical organic materials. Therefore, the thermal stabilities of the push–pull arylthienothiophene derivatives **9** and **10** were determined by thermogravimetric analysis (TGA), performed at a heating rate of 20 °C min^{-1} under nitrogen. The results obtained revealed the exceptional thermal stability of the dicyanovinyl push–pull derivatives **9**, which have decomposition temperatures (T_d) in the range 366–412 °C. Substitution of the dicyanovinyl acceptor group in **9** by the thiobarbituric moiety in **10** led to lower decomposition temperatures of 253–335 °C. These results are in agreement with earlier reports in which good to excellent thermal stabilities were communicated for other nonlinear optical thienothiophene derivatives.[11a,11c,11d,11e]

Photophysical Properties

The photophysical properties of all the push–pull derivatives were investigated in chloroform. The experimental data are presented in Table 4.

Absorption

As shown in Table 4, all the compounds show an intense absorption band in the near-UV or visible region, which can be ascribed to an intramolecular charge-transfer (ICT) transition. As expected, the nature of the donor and acceptor end groups significantly influences the position of this low-energy absorption band. Increasing the donor strength induces a progressive bathochromic shift, as illustrated in Figure 1 for series **8a**–**e** and also observed for series **9a**–**d** and **10a**,**b**,**d** (see Table 4).

Table 4. Photophysical and two-photon absorption properties of the TT derivatives **8a**–**e**, **9a**–**d**, and **10a**,**b**,**d** in chloroform.

	λ_{abs}^{max} [nm]	ε^{max} [10^4 M^{-1} cm^{-1}]	FWHM [10^3 cm^{-1}][a]	λ_{em}^{max} [nm]	Stokes shift [cm^{-1}]	Φ_f[b]	$\varepsilon^{max}\Phi_f$[c] [M^{-1} cm^{-1}]	τ[d] [ns]	$2\lambda_{abs}^{max}$ [nm]	λ_{TPA}^{max1} [nm]	$\sigma_2^{max1}\Phi_f$ [GM][e]	σ_2^{max1} [GM][f]
8a	358	3.6	4.5	413	3720	0.02[g–i]	7.2×10^2	0.12	716	–	–	–
8b	372	3.5	4.5	447	4510	0.58[g] 0.64[h,i]	2.1×10^4	1.26	744	750	50	82
8c	374	3.5	4.4	453	4660	0.65[g] 0.71[h,i]	2.4×10^4	1.44	748	750	60	88
8d	428	3.9	4.2	543	4950	0.87[h,i]	3.4×10^4	2.45	856	850	240	276
8e	428	2.8	4.2	545	5020	0.86[h,i]	2.4×10^4	2.44	856	850	180	209
9a	436	5.3	3.4	491	2570	0.002[h–j]	106	0.3	872	890	0.2	100
9b	455	3.9	3.6	531	3150	0.006[h–j]	234	0.2	910	940	1.4	233
9c	457	5.1	3.6	532	3080	0.007[g] 0.006[i,j]	331	0.1	914	960	2.4	369
9d	534	5.4	3.5	652	3390	0.61[i,j]	3.3×10^4	2.2	1068	1080	510	836
10a	495	7.2	2.8	548	1950	0.003[i,j]	216	0.84	990	–	–	–
10b	514	7.7	2.9	579	2180	0.006[i,j]	462	0.13	1028	1050	2.4	400
10d	595	7.6	3.0	710	2720	0.20[i] 0.19[j]	1.5×10^4	0.78	1190	≥1160	≥150	≥750

[a] Full width at half maximum. [b] Fluorescence quantum yield. [c] Brightness. [d] Experimental fluorescence lifetime. [e] Molecular TPEF action cross-section (i.e., two-photon brightness) at λ_{TPA}^{max}. [f] Molecular TPA cross-section at λ_{TPA}^{max}. 1 GM = 10^{-50} cm^4 s photon^{-1}. [g] Standard: quinine in 0.5 M H_2SO_4 (Φ_f = 0.546). [h] Standard: fluorescein in 0.1 M aq. NaOH (Φ_f = 0.90). [i] Standard: Rhodamine 6G in EtOH (Φ_f = 0.94). [j] Standard: Cresyl Violet in methanol (Φ_f = 0.54).

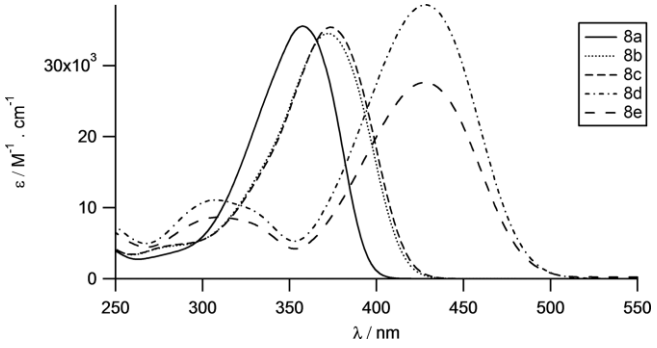

Figure 1. Absorption spectra of compounds **8a**–**e** in chloroform.

A marked batho- and hyperchromic shift as well as a narrowing of the main absorption band (Table 4) is observed on increasing the electron-withdrawing strength of the acceptor, as indicated by comparison of the absorption spectra of compounds **8**–**10d** (see Figure 2) and **8**–**10b** (see Figure S1 in the Supporting Information). These combined effects point to an increased polarization of the ground state (related to a larger contribution of the ICT mesomeric form in the description of the electronic structure) shifting the electronic structure towards a more "cyanine-like" structure.[28]

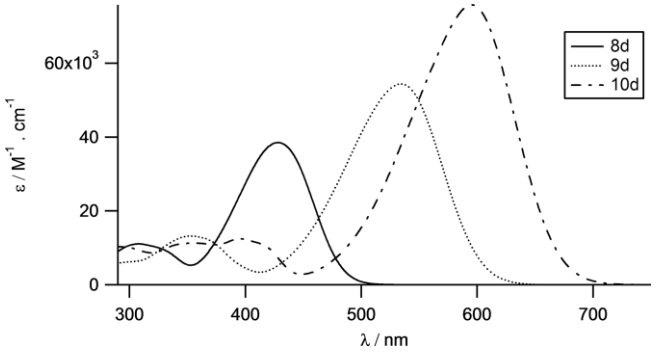

Figure 2. Absorption spectra of compounds **8**–**10d** in chloroform.

Fluorescence

As noted in Table 4, a number of the push–pull derivatives with a TT π-connector investigated in the present work show significant fluorescence. The fluorescence quantum yield was found to depend drastically on the nature of the acceptor and donor end groups. Indeed, all derivatives of series **8** (i.e., push–pull derivatives bearing an aldehyde as acceptor) except for **8a** (lacking the presence of a donor) show significant fluorescence quantum yields. In contrast to the derivatives of series **9** and **10** bearing strong acceptor end groups (i.e., dicyano or diethylthiobarbiturate), only compounds **9d** and **10d** bearing the strongest donor (i.e., dialkylamino) show sizeable quantum yields. Such behavior was observed earlier in related homologous compounds having a thiophene or bithiophene unit instead of TT.[20b] This behavior can be related to the nature of the lowest-energy excited state (responsible for emission): For stronger donor and acceptor end groups, the ICT π–π* transition shifts to lower energy, and the corresponding excited state is thus located below that of the n–π* transition (the band of which is hidden by the more intense ICT band). For compounds of series **9** and **10** with weaker donors (OMe, OEt), the n–π* transition is most probably found at a slightly lower energy and is thus responsible for only weak fluorescence (due to the reduced transition dipole). We note that compounds **9d** and **10d** show increased fluorescence quantum yields compared with their homologues having one or two thiophene units instead of a TT-connecting unit (Φ_f = 0.61 for **9d** instead of 0.13 and 0.34, and Φ_f = 0.20 for **10d** instead of 0.09 and 0.06). This enhanced fluorescence can be ascribed to both a higher radiative rate and a lower nonradiative rate. Hence, the planarization induced by the TT unit induces both higher transition dipoles and increases rigidity, both responsible for improved fluorescence efficiency. As a result, compounds **9d** and **10d** show much stronger brightness than their homologues with a thiophene or bithiophene instead of TT ($\varepsilon_{max}\Phi_f$ = 3.3×10^4 $M^{-1}\,cm^{-1}$ for dye **9d** compared with 1.3×10^4 $M^{-1}\,cm^{-1}$ for its bithiophene homologue[20b] and $\varepsilon_{max}\Phi_f$ = 1.5×10^4 $M^{-1}\,cm^{-1}$ for the dye **10d** compared with 2.6×10^3 $M^{-1}\,cm^{-1}$ compared with its bithiophene homologue),[20b] whereas their emission maxima are between those of the two homologues (i.e., redshifted compared with the homologue having one thiophene in the π-system and blueshifted compared with that of the homologue having two thiophene units).

The nature of the donor and acceptor end groups also significantly influences the fluorescence spectra. In all series, increasing the strength of the donor end group induces a progressive redshift of the emission spectrum, as illustrated in Figure 3 for series **8a**–**e**. In all cases an increase in the Stokes shift is also observed (see Table 4), which indicates a more pronounced photoinduced ICT.

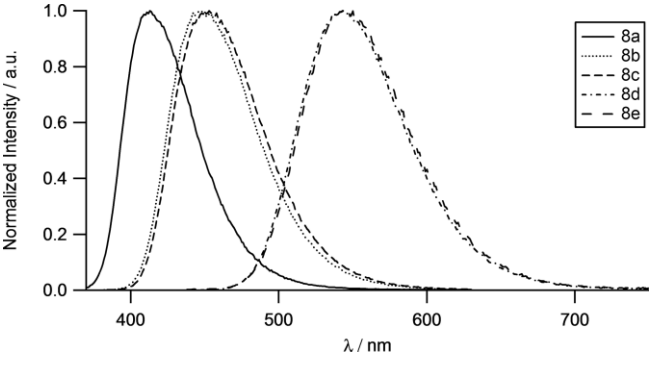

Figure 3. Emission spectra of compounds **8a**–**e** in chloroform.

Increasing the strength of the acceptor end group also induces a redshift of the emission, as shown in Figure 4 for series **8**–**10b** (and illustrated in Figure S2 in the Supporting Information for series **8**–**10d**). In both cases, however, we note a reduction of the Stokes shift (Table 4). This effect concomitant with a narrowing of the ICT absorption band and redshifts of both the emission and absorption bands points to a shift of the electronic structure of the dye towards the cyanine limit (with an increasing contribution of the zwitterionic mesomeric form to the description of the ground-state structure). Compound **10d**, which has the highest extinction coefficient, narrowest absorp-

tion band, smallest Stokes shift, and the most redshifted absorption and emission (with maximum located in the NIR region), is the closest to a cyanine-like structure.

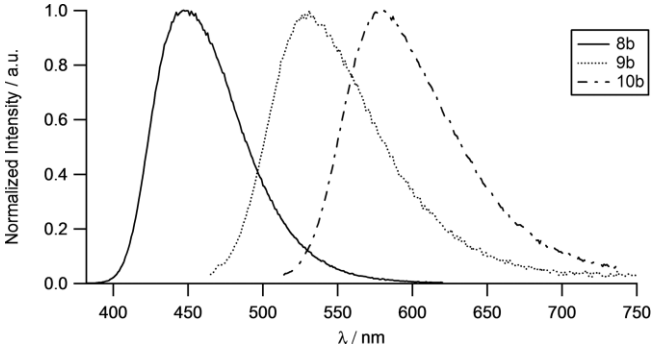

Figure 4. Emission spectra of compounds **8**–**10b** in chloroform.

Finally, we note that, whereas dyes **8b**–**e** are either blue (**8b**,**c**) or green (**8d**,**e**) bright emitters (with brightness values ranging between 2.1×10^4 and 3.4×10^4 M^{-1} cm^{-1}), dyes **9d** and **10d** are complementary bright red and NIR emitters.

Two-Photon Absorption

Owing to their fluorescence properties, the TPA of most push–pull derivatives can be determined by investigating their two-photon-induced fluorescence in solution. TPA spectra were recorded in the 700–1200 nm spectral range through femtosecond two-photon excited fluorescence experiments and by applying the methodology described by Webb and co-workers.[28] The corresponding data are presented in Table 4. All the compounds show a broad TPA band (Figures 5–7), the maxima of which are located at about twice the wavelength of the one-photon absorption (OPA) band, which indicates that the lowest excited state is both one- and two-photon-allowed, as expected for push–pull derivatives (see Figures S3–S5 in the Supporting Information). We stress that most probably the TPA properties of these dipolar derivatives are influenced by the solvent polarity, as reported recently for other dipolar heterocyclic derivatives.[10p] Here we chose a solvent of medium polarity in which to conduct the experiments.

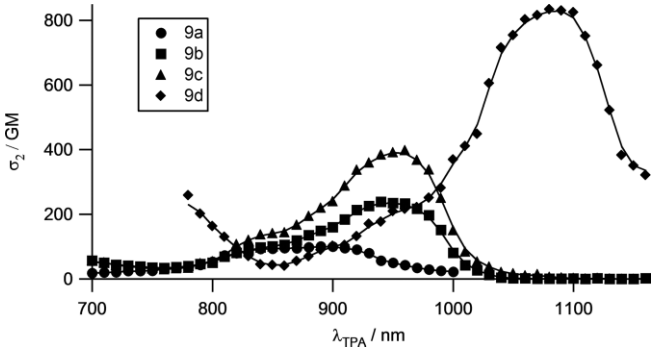

Figure 5. Two-photon absorption spectra of compounds **9a**–**d** in chloroform.

As illustrated in Figure 5, for series **9a**–**d**, increasing the strength of the donating end group induces both a redshift of the TPA band in the NIR region and pronounced enhancement of the maximum TPA cross-section. Such an effect is also observed for the series **8b**–**d** and **10b**,**d** (see Table 4 and the Supporting Information). As the fluorescence quantum yields also increase, the push–pull compounds bearing the strongest donating end group (i.e., the dialkylamino moiety) are found to produce the largest two-photon brightness: 240 GM for green-yellow emitter **8d**, 510 GM for red emitter **9d**, and 150 GM for NIR emitter **10d**.

Increasing the strength of the acceptor end group also induces a redshift of the TPA band, as illustrated in Figure 6 for series **8**–**10b** and Figure 7 for series **8**–**10d**. In the case of the series bearing an MeO donor end group (**8**–**10b**), the strongest acceptor (diethylthiobarbiturate) leads to the largest maximum TPA cross-section, whereas in the case of the series bearing the NEt_2 donor end group (**8**–**10d**), the maximum TPA cross-section is attained with the push–pull derivative bearing a dicyano acceptor (836 GM). This may be related to the electronic structure of dye **10d**, which is much closer to the cyanine limit than **9d** and thus leads to a lower TPA response.[29] In addition, we note that in the case of the diethylthiobarbiturate acceptor, steric hindrance due to the repulsion between the lone pairs of the sulfur atom of the thiophene ring and the oxygen atoms of the acceptor may cause deviation from planarity, which may also influence the TPA properties.

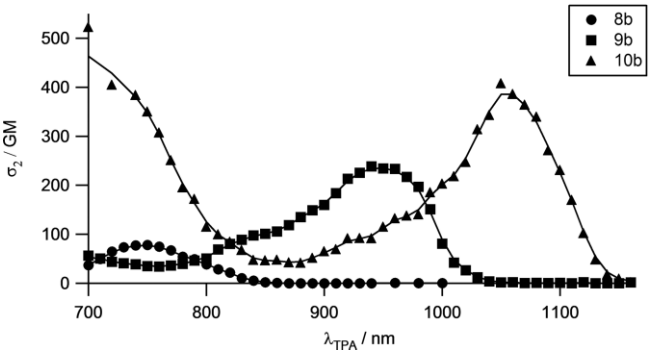

Figure 6. Two-photon absorption spectra of compounds **8**–**10b** in chloroform.

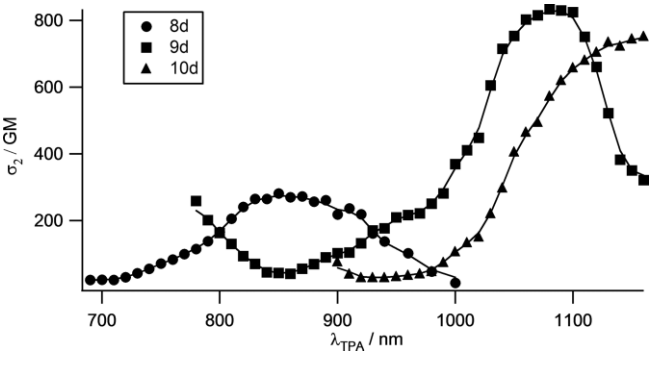

Figure 7. Two-photon absorption spectra of compounds **8**–**10d** in chloroform.

Finally, it is of interest to compare the two-photon absorption response of the brightest two-photon dyes (i.e., **8d**, **9d**, and **10d**) with those of their homologues having a bithiophene π-connector instead of a TT π-connector in the conjugated

path.[20b] The aldehyde derivative **8d** shows a slightly larger TPA maximum cross-section (276 GM compared with 253 GM), whereas the dicyanovinyl derivative **9d** shows a much larger TPA maximum cross-section (836 GM compared with 570 GM), whereas the thiobarbituric acid derivative **10d** shows a smaller TPA maximum cross-section (750 GM compared with 1600 GM).

This trend can be interpreted by the different polarization of the derivatives bearing different acceptor end groups. Increasing the acceptor strength leads to increased polarization, as mentioned above. Replacing the bithiophene π-connector by the TT π-connector also increases the polarization and shifts the electronic structure closer to the cyanine limit. This is due to the reduced aromaticity of the TT unit compared with that of the bithiophene (leading to a lower gap *V*[29]). In addition, the planarity of the TT moiety (as compared with the free rotation of the single bond linking the two thiophene rings in the bithiophene π-connector) favors coupling and thus also shifts the structure closer to the cyanine limit. The narrower ICT absorption bands of compounds **8**–**10d** as compared with those of their analogues having a bithiophene π-connector[20b] provides clear evidence for this effect. Because there is an optimum electronic distribution (positioned between the neutral form and the cyanine limit) that maximizes the TPA response of push–pull derivatives, the effect of increased polarization depends on the initial polarization.[29] Owing to the low initial polarization in the aldehyde derivatives (i.e., derivatives **8**), the effect of the TT is favorable as it increases the polarization and shifts the structure closer to the optimum polarization. This effect is even more pronounced for the dicyanovinyl derivatives, which is most probably very close to the optimum polarization leading to a maximum TPA response for compound **9d**. In contrast, owing to the strong electron-withdrawing strength of the diethylthiobarbiturate, the electronic distribution in **10** is close to the cyanine limit (i.e., past the optimum polarization), thus leading to a decrease in the TPA response on increasing the polarization.

In any case, owing to their much higher fluorescence quantum yields, compounds **8**–**10d** show improved two-photon brightness in comparison with their homologues having bithiophene instead of TT in the conjugated system. This demonstrates that the strategy implemented herein is of major interest for the design of series of bright fluorescent dyes showing tunable emission in the visible region down to the NIR region and high two-photon brightness. In particular, the fluorescent dye **10d** offers major promise as it can be both two-photon-excited in the NIR region (close to 1.2 μm) and emits in the NIR region. As such, it holds promise as a novel fluorochrome for biological imaging.

Conclusions

5-Arylthieno[3,2-*b*]thiophene-2-carbaldehydes **8** have been synthesized by the Suzuki coupling reaction of functionalized arylboronic acids with 5-bromothieno[3,2-*b*]thiophene-2-carbaldehyde (**6**). Donor–acceptor-substituted thieno[3,2-*b*]thiophenes **9** and **10** were then prepared in moderate to good yields from the formyl-substituted derivatives **8** and low-cost commercially available reagents by using simple and convenient synthetic methodologies.

These new derivatives were found to show intense absorption in the near-UV through to the orange visible region depending on the nature of the donor and acceptor end groups, which can be ascribed to strong ICT transitions. Although all the push–pull aldehydes show good fluorescence properties, only the push–pull derivatives combining a strong acceptor (i.e., dicyanovinyl or diethylthiobarbiturate) and stronger donor (dialkylamino) show sizeable fluorescence. In addition, these derivatives were found to show both improved fluorescence quantum yields compared with their homologues with a bithiophene instead of a TT moiety in the conjugated π-system as well as a stronger TPA response. As a result, by using the fused thiophene conjugated system, several new fluorescent dyes showing enhanced one- and two-photon brightness and tunable emission (i.e., blue, green, red, and NIR) have been obtained. These dyes hold promise as new fluorescent probes for bioimaging purposes.

Experimental Section

Synthesis: TLC was carried out on 0.25 mm precoated silica plates (Merck Fertigplatten Kieselgel 60F_{254}). Melting points were measured with a Gallenkamp melting-point apparatus. NMR spectra were recorded with a Varian Unity Plus spectrometer at an operating frequency of 300 MHz for ^{1}H NMR and 75.4 MHz for ^{13}C NMR or a Bruker Avance III 400 spectrometer at an operating frequency of 400 MHz for ^{1}H NMR and 100.6 MHz for ^{13}C NMR using the solvent peak as internal reference at 25 °C. All chemical shifts are given in ppm using Me_4Si as reference (δ_H = 0 ppm), and *J* values are given in Hz. Assignments were made by comparison of chemical shifts, peak multiplicities, and *J* values, and were supported by spin-decoupling double resonance and 2-dimensional heteronuclear HMBC and HMQC correlation techniques. IR spectra were recorded with an FTIR Perkin–Elmer 1600 spectrophotometer in Nujol or KBr. Elemental analyses were performed with a Leco CHNS 932 instrument. Low- and high-resolution mass spectrometry was performed at the "C.A.C.T.I. – Unidad de Espectrometria de Masas" at the University of Vigo, Spain. All Suzuki coupling reactions were carried out under argon, and all commercially available reagents and solvents were used as received.

Synthesis of 3-Bromothiophene-2-carbaldehyde (2): 3-Bromothiophene (**1**; 29.35 g, 180 mmol) was added dropwise to a stirred solution of lithium diisopropylamide [LDA; prepared by the addition of butyllithium (2.5 mol L^{-1} in hexane; 80 mL, 200 mmol) to diisopropylamine (22.24 g, 220 mmol)] in dry THF (300 mL) at 0 °C, and the resulting mixture was stirred at this temperature for a further 30 min prior to the addition of DMF (16.3 mL, 15.3 g, 210 mmol). The mixture was stirred for 3 h when an excess of 20 % aqueous ammonium chloride was added. The product was extracted with diethyl ether (3 × 250 mL), washed with water (3 × 300 mL), and dried with magnesium sulfate. Evaporation of the organic solvent gave 34.4 g (180 mmol) of 3-bromothiophene-2-carbaldehyde (**2**)[24] in quantitative yield as a brown oil. ^{1}H NMR ($CDCl_3$): δ = 7.13 (d, *J* = 5.1 Hz, 1 H), 7.70 (dd, *J* = 5.1, 1.4 Hz, 1 H), 9.95 (d, *J* = 1.4 Hz, 1 H, CHO) ppm.

Synthesis of Methyl Thieno[3,2-*b*]thiophene-2-carboxylate (3): 3-Bromothiophene-2-carbaldehyde (**2**; 34.4 g, 180 mmol) was

added to a stirred mixture of methyl 2-sulfanylacetate (16.1 mL, 19.10 g, 180.0 mmol), potassium carbonate (37.3 g), and DMF (140 mL) at room temperature, and the resulting mixture was stirred at 60 °C for 72 h. Then it was poured into water (600 mL), and the precipitate was filtered to give 21.4 g of methyl thieno[3,2-*b*]-thiophene-2-carboxylate (**3**)[24] as a yellow solid in 60 % yield. M.p. 95–96 °C. ^{1}H NMR ($CDCl_3$): δ = 3.91 (s, 3 H), 7.27 (d, J = 5.3 Hz, 1 H), 7.58 (d, J = 5.3 Hz, 1 H), 7.99 (s, 1 H) ppm.

Synthesis of 2-(Hydroxymethyl)thieno[3,2-*b*]thiophene (4): A solution of methyl thieno[3,2-*b*]thiophene-2-carboxylate (**3**; 15 g, 75.7 mmol) in dry diethyl ether (350 mL) was added during 2 h to a suspension of lithium aluminium hydride (5.75 g, 151.5 mmol) in dry diethyl ether (200 mL) that had been cooled in an ice/water bath. After the addition was complete, the mixture was stirred at room temperature for 3 h. The reaction mixture was worked up by cooling in an ice/water bath with successive dropwise addition of water (5.7 mL), 15 % aqueous sodium hydroxide (6 mL), and water (18 mL) with vigorous stirring. Vigorous stirring was continued until the salts were well granulated. The diethyl ether solution of the product was decanted, and the salts were washed with diethyl ether. Both diethyl ether solutions were dried with $MgSO_4$ and filtered, and the solvent was evaporated under vacuum to give 11.6 g of product **4** as a white solid[25] in 90 % yield. ^{1}H NMR ($CDCl_3$): δ = 4.87 (s, 2 H), 7.19 (s, 1 H), 7.22 (d, J = 5.2 Hz, 1 H), 7.34 (d, J = 5.2 Hz, 1 H) ppm. ^{13}C NMR ($CDCl_3$): δ = 61.0, 117.8, 119.6, 127.0, 139.2, 146.1 ppm.

Synthesis of Thieno[3,2-*b*]thiophene-2-carbaldehyde (5): A solution of 2-(hydroxymethyl)thieno[3,2-*b*]thiophene (**4**; 11.6 g, 68.3 mmol) in dichloromethane (160 mL) was added in one portion to a stirred suspension of pyridinium chlorochromate (PCC; 22.1 g, 102.4 mmol), the PCC having been ground with a pestle in a mortar and partially dissolved in dichloromethane with vigorous stirring. Stirring was continued for 2 h. Further PCC (5.9 g, 27.3 mmol) was added, and the mixture was stirred vigorously for 30 min. The solution was worked up by adding diethyl ether (1 L) and then filtering through a column of silica gel. The gum in the flask was washed with diethyl ether (3 × 1500 mL), and these washings were passed through the column of silica gel. The solvents were evaporated under vacuum to give 8.37 g of a dark-purple crude product, which was recrystallized from cyclohexane to give the pure compound as a pale-gray solid. M.p. 51–52 °C (ref.[25] m.p. 53–54 °C). ^{1}H NMR ($CDCl_3$): δ = 7.33 (d, J = 5.2 Hz, 1 H), 7.47 (d, J = 5.2 Hz, 1 H), 7.92 (s, 1 H), 9.98 (s, 1 H, CHO) ppm.

Synthesis of 5-Bromothieno[3,2-*b*]thiophene-2-carbaldehyde (6): Thieno[3,2-*b*]thiophene-2-carbaldehyde (**5**; 8.37 g, 49.8 mmol) was dissolved in chloroform (150 mL). Sodium hydrogen carbonate (4.6 g) was added to the solution, which was cooled to 0 °C. Bromine (2.56 mL, 8.0 g, 49.8 mmol) was added dropwise, and the mixture was stirred at room temperature for 2 h. The organic layer was extracted with water (200 mL), and the aqueous phase was extracted with dichloromethane (3 × 150 mL). The organic solutions were combined, dried with magnesium sulfate, and the solvents evaporated under vacuum to leave a dark solid, which was recrystallized from cyclohexane to give 9.4 g (88 %) of 5-bromothieno-[3,2-*b*]thiophene-2-carbaldehyde (**6**)[14b,26] as a gray solid. M.p. 142–143 °C. IR (Nujol): $\tilde{\nu}$ = 1660, 1409, 1336, 1301, 1280, 1264, 1225, 1148, 1122, 990, 977, 853, 829, 807, 790, 738, 722, 694, 658, 630 cm^{-1}. ^{1}H NMR ($CDCl_3$): δ = 7.34 (s, 1 H), 7.83 (s, 1 H), 9.96 (s, 1 H, CHO) ppm. ^{13}C NMR ($CDCl_3$): δ = 120.9, 122.9, 128.2, 139.3, 144.5, 144.7, 183.3 ppm. MS (EI): m/z (%) = 247 (63) [M]$^+$ (^{81}Br), 245 (66) [M]$^+$ (^{79}Br), 219 (6), 218 (13), 217 (7), 216 (11), 139 (13), 138 (20), 95 (9), 93 (16), 81 (4), 69 (100). HRMS (EI): calcd. for $C_7H_3{}^{79}BrOS_2$ 245.8809; found 245.8810; calcd. for $C_7H_3{}^{81}BrOS_2$ 247.8788; found 247.8790.

General Procedures for the Suzuki Coupling Reactions

Method A: 5-Bromothieno[3,2-*b*]thiophene-2-carbaldehyde (**6**; 0.25 mmol, 100 mg) was coupled with boronic acids **7a**–**e** (0.33 mmol) in a mixture of DME (6 mL), an aqueous solution of Na_2CO_3 (0.4 mL, 2 M), and [$Pd(PPh_3)_4$] (6 mol-%) at 80 °C under nitrogen. The reactions were monitored by TLC, which determined the different reaction times (4–24 h). After cooling, the mixture was filtered, and ethyl acetate and a saturated solution of NaCl were added, and the phases were separated. The organic phase was washed with water (3 × 10 mL) and a solution of 10 % NaOH (1 × 10 mL). The organic phase obtained was dried with $MgSO_4$, filtered, and the solvent removed under vacuum to give the crude mixture of products, which were submitted to column chromatography on silica gel with increasing amounts of diethyl ether in light petroleum as eluent to afford the pure products **8a**–**e**.

Method B: 5-Bromothieno[3,2-*b*]thiophene-2-carbaldehyde (**6**; 0.25 mmol, 100 mg) was coupled to boronic acids **7a**–**e** (0.33 mmol) in a mixture of toluene (6 mL), K_2CO_3 (2.5 mmol, 0.64 g, 10 equiv.), ethanol (3.2 mL), water (1 mL), and [$Pd(PPh_3)_4$] (10 mol-%) at reflux under nitrogen. The reactions were monitored by TLC, which determined the different reaction times (1–2 h). After cooling, the mixture was filtered, and the solid was washed with CH_2Cl_2. The organic phase obtained was washed with water (3 × 10 mL), dried with $MgSO_4$, filtered, and the solvent removed under vacuum to give the crude products, which were submitted to column chromatography on silica gel with dichloromethane as eluent to afford the coupled products **8a**–**e**. Recrystallization from dichloromethane/petroleum ether gave the pure compounds.

5-Phenylthieno[3,2-*b*]thiophene-2-carbaldehyde (8a): Yellow solid (Method A, 35 % yield; Method B, 80 % yield). M.p. 165–166 °C. ^{1}H NMR (300 MHz, $CDCl_3$): δ = 7.39–7.49 (m, 3 H, 4′-H, 3′-H, 5′-H), 7.55 (s, 1 H, 6-H), 7.67–7.69 (m, 2 H, 2′-H, 6′-H), 7.93 (s, 1 H, 3-H), 9.97 (s, 1 H, C*H*O) ppm. ^{13}C NMR (75.4 MHz, $CDCl_3$): δ = 115.8, 126.2, 129.0, 129.2, 133.7, 138.2, 144.5, 146.7, 152.9, 181.2 ppm. IR (Nujol): $\tilde{\nu}$ = 3094, 3059, 2851, 1662, 1625, 1513, 1498, 1259, 1021 cm^{-1}. MS (EI): m/z (%) = 245 (15) [M + 1]$^+$, 244 (100) [M]$^+$, 243 (61), 216 (14), 215 (17), 171 (33), 145 (12), 93 (17). HRMS (EI): calcd. for $[C_{13}H_8OS_2]^+$ 244.0017; found 244.0021.

5-(4-Methoxyphenyl)thieno[3,2-*b*]thiophene-2-carbaldehyde (8b): Yellow solid (Method A, 50 % yield; Method B, 72 % yield). M.p. 169–170 °C. ^{1}H NMR (300 MHz, $CDCl_3$): δ = 3.87 (s, 3 H, OCH_3), 6.96 (d, J = 6.9 Hz, 2 H, 3′-H, 5′-H), 7.41 (d, J = 0.6 Hz, 1 H, 6-H), 7.59 (d, J = 6.9 Hz, 2 H, 2′-H, 6′-H), 7.88 (d, J = 0.6 Hz, 1 H, 3-H), 9.94 (s, 1 H, C*H*O) ppm. ^{13}C NMR (75.4 MHz, $CDCl_3$): δ = 55.4, 114.6, 126.5, 127.6, 129.3, 137.5, 144.0, 147.0, 153.1, 160.4, 183.1 ppm. IR (Nujol): $\tilde{\nu}$ = 3091, 3047, 2980, 2851, 1660, 1603, 1523, 1462, 1262, 1024 cm^{-1}. MS (EI): m/z (%) = 275 (11) [M + 1]$^+$, 274 (60) [M]$^+$, 259 (47), 231 (8), 203 (14), 149 (9), 137 (20), 123 (14), 121 (17), 109 (12), 95 (21), 93 (7), 81 (63), 69 (100). HRMS (EI): calcd. for $[C_{14}H_{10}O_2S_2]^+$ 274.0122; found 274.0122.

5-(4-Ethoxyphenyl)thieno[3,2-*b*]thiophene-2-carbaldehyde (8c): Yellow solid (Method A, 85 % yield; Method B, 79 % yield). M.p. 175–176 °C. ^{1}H NMR (250 MHz, $CDCl_3$): δ = 1.37 (t, J = 7.0 Hz, 3 H, OCH$_2$$CH_3$), 4.09 (q, J = 7.0 Hz, 2 H, OCH_2CH$_3$), 6.95 (d, J = 8.8 Hz, 2 H, 3′-H, 5′-H), 7.42 (s, 1 H, 6-H), 7.58 (d, J = 8.8 Hz, 2 H, 2′-H, 6′-H), 7.90 (s, 1 H, 3-H), 9.94 (s, 1 H, C*H*O) ppm. ^{13}C NMR (62.9 MHz, $CDCl_3$): δ = 14.8, 63.7, 115.1, 126.3, 127.6, 129.3, 137.5, 144.0, 147.1, 153.3, 159.8, 183.1 ppm. IR (Nujol): $\tilde{\nu}$ = 3091, 3050, 2978, 2850, 1650, 1605, 1523, 1469, 1259, 1044 cm^{-1}. MS (EI): m/z (%) = 289 (15) [M + 1]$^+$, 288 (98) [M]$^+$, 262 (11), 261 (22), 260 (88), 259 (100), 233 (6), 232 (14), 203 (19), 187 (11), 171 (12), 158 (9). HRMS (EI): calcd. for $[C_{15}H_{12}O_2S_2]^+$ 288.0279; found 288.0285.

5-[4-(Diethylamino)phenyl]thieno[3,2-*b*]thiophene-2-carbaldehyde (8d): Orange solid (Method A, 36 % yield; Method B, 84 % yield). M.p. 202–203 °C. ^{1}H NMR (300 MHz, [D$_6$]DMSO): δ = 1.13 [t, J = 6.9 Hz, 6 H, N(CH$_2$C*H*$_3$)$_2$], 3.40 [q, J = 6.9 Hz, 4 H, N(C*H*$_2$CH$_3$)$_2$], 6.74 (d, J = 9.0 Hz, 2 H, 3′-H, 5′-H), 7.52 (d, J = 9.0 Hz, 2 H, 2′-H, 6′-H), 7.65 (s, 1 H, 6-H), 8.25 (s, 1 H, 3-H), 9.91 (s, 1 H, C*H*O) ppm. ^{13}C NMR (75.4 MHz, [D$_6$]DMSO): δ = 12.1, 43.4, 111.6, 112.8, 119.8, 126.8, 130.5, 135.8, 142.5, 146.3, 147.9, 153.6, 183.3 ppm. IR (Nujol): $\tilde{\nu}$ = 3089, 2892, 2803, 1655, 1602, 1552, 1430, 1355 cm^{-1}. MS (EI): *m/z* (%) = 316 (7) [M + 1]$^+$, 315 (39) [M]$^+$, 300 (100), 271 (28), 243 (7), 171 (8), 150 (4). HRMS (EI): calcd. for [C$_{17}$H$_{17}$NOS$_2$]$^+$ 315.0752; found 315.0750.

5-[4-(Pyrrolidin-1-yl)phenyl]thieno[3,2-*b*]thiophene-2-carbaldehyde (8e): Orange solid (Method A, 30 % yield; Method B, 70 % yield). M.p. >250 °C. ^{1}H NMR (300 MHz, [D$_6$]DMSO): δ = 1.94–1.99 [m, 4 H, N(CH$_2$C*H*$_2$)$_2$], 3.26–3.28 [m, 4 H, N(C*H*$_2$CH$_2$)$_2$], 6.61 (d, J = 8.7 Hz, 2 H, 3′-H, 5′-H), 7.55 (d, J = 8.7 Hz, 2 H, 2′-H, 6′-H), 7.73 (s, 1 H, 6-H), 8.31 (s, 1 H, 3-H), 9.90 (s, 1 H, C*H*O) ppm. ^{13}C NMR (100 MHz, [D$_6$]DMSO): δ = 24.9 [N(CH$_2$*C*H$_2$)$_2$], 47.3 [N(*C*H$_2$CH$_2$)$_2$], 112.0 (C-6), 113.1 (C-3′, C-5′), 120.1 (C-1′), 127.0 (C-2′, C-6′), 131.4 (C-3), 136.0 (C-5), 142.6 (C-3a or C-6a), 146.7 (C-6a or C-3a), 148.2 (C-2), 154.1 (C-4′), 184.0 (*C*HO) ppm. IR (Nujol): $\tilde{\nu}$ = 3088 (νCH-Ar), 2980 (νCH-Aliph), 2803 (νCH-Ald), 1657 (νC=O), 1607, 1530 (νC=C), 1432 (νCH), 1357 (νC–N) cm^{-1}. MS (EI): *m/z* (%) = 314 (25) [M + 1]$^+$, 313 (100) [M]$^+$, 309 (61), 285 (5), 280 (13), 270 (9), 257 (21), 171 (14), 93 (10), 84 (5). HRMS (EI): calcd. for [C$_{17}$H$_{15}$NOS$_2$]$^+$ 313.0595; found 313.0599.

General Procedure for the Synthesis of Dicyanovinyl-arylthienothiophene Derivatives 9 from the Corresponding Formyl Precursors 8 by Knoevenagel Condensation with Malononitrile: Piperidine (1 drop) was added to a solution of malononitrile (0.08 g, 1.2 mmol) and aldehyde **8** (1.0 mmol) in dichloromethane (25 mL). The solution was stirred at room temperature for different reaction times (15 min to 3 h), petroleum ether (200 mL) was added, and the resulting precipitate of the dicyanovinyl derivative **9** was filtered. The crude compounds were submitted to silica gel column chromatography using mixtures of chloroform and light petroleum of increasing polarity. The fraction containing the purified product was collected and the solvent evaporated under vacuum. Recrystallization from dichloromethane/petroleum ether gave the pure compounds.

2-[(5-Phenylthieno[3,2-*b*]thiophen-2-yl)methylene]malononitrile (9a): Orange solid (132 mg, 54 %). M.p. 245–246 °C. ^{1}H NMR (300 MHz, [D$_6$]DMSO): δ = 7.41–7.53 (m, 3 H, 3′-H, 4′-H, 5′-H), 7.77 (d, J = 6.9 Hz, 2 H, 2′-H, 6′-H), 8.08 (s, 1 H, 6-H), 8.27 (s, 1 H, 3-H), 8.76 [s, 1 H, C*H*=C(CN)$_2$] ppm. ^{13}C NMR (75.4 MHz, [D$_6$]DMSO): δ = 74.2, 114.0, 114.7, 117.1, 126.0, 129.5, 129.6, 133.1, 133.8, 136.4, 138.4, 148.4, 153.6 ppm. IR (Nujol): $\tilde{\nu}$ = 3020, 2948, 2216, 1606, 1509, 1413 cm^{-1}. MS (EI): *m/z* (%) = 293 (100) [M]$^+$, 277 (32), 263 (30), 237 (31), 226 (56), 203 (11). HRMS (EI): calcd. for [C$_{16}$H$_9$N$_2$S$_2$]$^+$ 293.0202; found 293.0203.

2-{[5-(4-Methoxyphenyl)thieno[3,2-*b*]thiophen-2-yl]methylene}malononitrile (9b): Red solid (134 mg, 49 %). M.p. 212–213 °C. ^{1}H NMR (300 MHz, [D$_6$]DMSO): δ = 3.82 (s, 3 H, OC*H*$_3$), 7.06 (d, J = 8.8 Hz, 2 H, 3′-H, 5′-H), 7.71 (d, J = 6.8 Hz, 2 H, 2′-H, 6′-H), 7.95 (s, 1 H, 6-H), 8.24 (s, 1 H, 3-H), 8.72 [s, 1 H, C*H*=C(CN)$_2$] ppm. ^{13}C NMR (75.4 MHz, [D$_6$]DMSO): δ = 55.4, 73.4, 114.1, 114.8, 115.6, 125.7, 127.6, 133.8, 135.8, 137.7, 148.9, 153.4, 160.4 ppm. IR (Nujol): $\tilde{\nu}$ = 3024, 2984, 2219, 1606, 1523, 1412, 1257, 1033 cm^{-1}. MS (EI): *m/z* (%) = 322 (100) [M]$^+$, 298 (23), 209 (15). HRMS (EI): calcd. for [C$_{17}$H$_{10}$N$_2$OS$_2$]$^+$ 322.0229; found 322.0228.

2-{[5-(4-Ethoxyphenyl)thieno[3,2-*b*]thiophen-2-yl]methylene}malononitrile (9c): Red solid (231 mg, 74 %). M.p. 236–237 °C. ^{1}H NMR (300 MHz, [D$_6$]DMSO): δ = 1.35 (t, J = 7.2 Hz, 3 H, OCH$_2$C*H*$_3$), 4.09 (q, J = 7.2 Hz, 2 H, OC*H*$_2$CH$_3$), 7.04 (d, J = 7.2 Hz, 2 H, 3′-H, 5′-H), 7.68 (d, J = 7.2 Hz, 2 H, 2′-H, 6′-H), 7.89 (s, 1 H, 6-H), 8.22 (s, 1 H, 6-H), 8.71 [s, 1 H, C*H*=C(CN)$_2$] ppm. ^{13}C NMR (75.4 MHz, [D$_6$]DMSO): δ = 14.2, 63.2, 73.3, 113.8, 114.5, 115.2, 125.4, 127.3, 133.1, 135.5, 137.5, 148.6, 152.9, 159.5 ppm. IR (Nujol): $\tilde{\nu}$ = 3021, 2971, 2221, 1609, 1485, 1414, 1259, 1051 cm^{-1}. MS (EI): *m/z* (%) = 336 (100) [M]$^+$, 274 (10), 209 (11). HRMS (EI): calcd. for [C$_{18}$H$_{12}$N$_2$OS$_2$]$^+$ 336.0386; found 336.0385.

2-({5-[4-(Diethylamino)phenyl]thieno[3,2-*b*]thiophen-2-yl}methylene)malononitrile (9d): Violet solid (154 mg, 81 %). M.p. 220–221 °C. ^{1}H NMR (400 MHz, [D$_6$]DMSO): δ = 1.11 [t, J = 7.0 Hz, 6 H, N(CH$_2$C*H*$_3$)$_2$], 3.40 [q, J = 7.0 Hz, 4 H, N(C*H*$_2$CH$_3$)$_2$], 6.73 (d, J = 8.8 Hz, 2 H, 3′-H, 5′-H), 7.55 (d, J = 8.8 Hz, 2 H, 2′-H, 6′-H), 7.79 (s, 1 H, 6-H), 8.17 (s, 1 H, 3-H), 8.63 [s, 1 H, C*H*=C(CN)$_2$] ppm. ^{13}C NMR (100 MHz, [D$_6$]DMSO): δ = 12.4, 43.8, 71.5, 111.6, 113.1, 115.2, 119.4, 127.5, 133.8, 134.8, 136.5, 148.5, 149.9, 152.9 ppm. IR (Nujol): $\tilde{\nu}$ = 3025, 2978, 2214, 1606, 1534, 1403, 1355 cm^{-1}. MS (EI): *m/z* (%) = 363 (100) [M]$^+$, 165 (5). HRMS (EI): calcd. for [C$_{20}$H$_{17}$N$_3$S$_2$]$^+$ 363.0858; found 363.0855.

General Procedure for the Synthesis of Arylthienothiophene Thiobarbituric Acid Derivatives 10a–c from the Corresponding Formyl Precursors 8 by Knoevenagel Condensation with Thiobarbituric Acid: Piperidine (1 drop) was added to a solution of 1,3-diethyl-2-thiobarbituric acid (80 mg, 0.38 mmol, 1.2 equiv.) and aldehyde **8** (0.32 mmol, 1.0 equiv.) in acetonitrile (20 mL). The solution was heated at reflux for 2–3 h and then cooled to 0 °C. The resulting precipitate of compound **8** was filtered, washed with diethyl ether (15 mL) and collected. Recrystallization from dichloromethane/petroleum ether gave the pure compounds.

1,3-Diethyl-5-[(5-phenylthieno[3,2-*b*]thiophen-2-yl)methylene]-2-thioxo-2,3-dihydropyrimidine-4,6(1*H*,5*H*)-dione (10a): Red solid (33 mg, 42 %). M.p. 227–228 °C. ^{1}H NMR (400 MHz, [D$_6$]DMSO): δ = 1.32–1.39 [m, 6 H, N(CH$_2$C*H*$_3$)$_2$], 4.57–4.66 [m, 4 H, N(C*H*$_2$CH$_3$)$_2$], 7.40–7.49 (m, 3 H, 3′-H, 4′-H, 5′-H), 7.56 (s, 1 H, 6-H), 7.71 (d, J = 6.8 Hz, 2 H, 2′-H, 6′-H), 8.08 (s, 1 H, 3-H), 8.75 (s, 1 H, C=C*H*) ppm. ^{13}C NMR (75.4 MHz, [D$_6$]DMSO): δ = 12.4, 12.5, 43.3, 44.0, 110.5, 115.8, 126.5, 129.3, 129.6, 133.6, 137.4, 139.3, 150.2, 155.2, 155.8, 159.8, 161.0, 178.6 ppm. IR (Nujol): $\tilde{\nu}$ = 3088, 1682, 1654, 1549, 1511, 1416, 1345 cm^{-1}. MS (EI): *m/z* (%) = 427 (5) [M + 1]$^+$, 391 (7), 364 (16), 339 (19), 310 (100), 279 (7), 192 (5), 153 (2). HRMS (EI): calcd. for [C$_{21}$H$_{18}$N$_2$O$_2$S$_3$ + H]$^+$ 427.0603; found 427.0602.

1,3-Diethyl-5-{[5-(4-methoxyphenyl)thieno[3,2-*b*]thiophen-2-yl]methylene}-2-thioxo-2,3-dihydropyrimidine-4,6(1*H*,5*H*)-dione (10b): Red solid (65 mg, 74 %). M.p. 249–250 °C. ^{1}H NMR (400 MHz, CDCl$_3$): δ = 1.33–1.37 [m, 6 H, N(CH$_2$C*H*$_3$)$_2$], 3.88 (s, 3 H, OC*H*$_3$), 4.59–4.64 [m, 4 H, N(C*H*$_2$CH$_3$)$_2$], 6.98 (d, J = 8.8 Hz, 2 H, 3′-H, 5′-H), 7.44 (s, 1 H, 6-H), 7.66 (d, J = 8.8 Hz, 2 H, 2′-H, 6′-H), 8.06 (s, 1 H, 3-H), 8.74 (s, 1 H, C=C*H*) ppm. ^{13}C NMR (100 MHz, CDCl$_3$): δ = 12.4, 12.5, 43.2, 44.0, 55.5, 109.9, 114.7, 126.3, 127.9, 137.5, 138.6, 138.9, 150.1, 155.9, 156.3, 159.8, 160.9 161.1, 178.6 ppm. IR (Nujol): $\tilde{\nu}$ = 3089, 2978, 1682, 1653, 1606, 1479, 1416, 1330, 1262, 1063 cm^{-1}. MS (EI): *m/z* (%) = 457 (6) [M + 1]$^+$, 401 (11), 371 (100), 299 (56), 223 (12). HRMS (EI): calcd. for [C$_{22}$H$_{20}$N$_2$O$_3$S$_3$ + H]$^+$ 457.0708; found 457.0709.

1,3-Diethyl-5-({5-[4-(diethylamino)phenyl]thieno[3,2-*b*]thiophen-2-yl}methylene)-2-thioxo-2,3-dihydropyrimidine-4,6(1*H*,5*H*)-dione (10d): Green solid (83 mg, 82 %). M.p. 238–239 °C. ^{1}H NMR (300 MHz, CDCl$_3$): δ = 1.25–1.28 [m, 6 H, N(CH$_2$C*H*$_3$)$_2$], 1.31–1.39 [m, 6 H, N(CH$_2$C*H*$_3$)$_2$], 3.46–3.51 [m, 4 H, N(C*H*$_2$CH$_3$)$_2$], 4.57–4.66 [m, 4 H, N(C*H*$_2$CH$_3$)$_2$], 6.44 (d, J = 8.7 Hz, 2

H, 3′-H, 5′-H), 7.66 (d, J = 8.7 Hz, 2 H, 2′-H, 6′-H), 8.04 (s, 1 H, 6-H), 8.54 (s, 1 H, 3-H), 8.67 (s, 1 H, C=C*H*) ppm. IR (Nujol): $\tilde{\nu}$ = 3073, 2931, 1681, 1655, 1602, 1545, 1405, 1351, 1328 cm^{-1}. MS (EI): m/z (%) = 497 (100) $[M]^+$. HRMS (EI): calcd. for $[C_{25}H_{27}N_3O_2S_3]^+$ 497.1260; found 497.1258. $C_{25}H_{27}N_3O_2S_3$ (497.70): calcd. C 60.33, H 5.47, N 8.44, S 19.33; found C 60.06, H 5.58, N 8.16, S 19.23.

Photophysical Studies: All the photophysical experiments were carried out with freshly prepared, air-equilibrated solutions at room temperature (293 K). UV/Vis absorption spectra were recorded using a Jasco V-570 spectrophotometer. Steady-state fluorescence measurements were performed on dilute solutions (optical density <0.1) contained in standard 1 cm quartz cuvettes using a Horiba (FluoroLog or FluoroMax) spectrometer in photon-counting mode. Fully corrected emission spectra were recorded for each compound at $\lambda_{ex} = \lambda_{abs}{}^{max}$ with an optical density at $\lambda_{ex} \leq 0.1$ to minimize internal absorption. Fluorescence quantum yields were measured according to literature procedures[30] using fluorescein in 0.1 M NaOH (Φ_f = 0.9), quinine bisulfate in 0.5 M H_2SO_4 (Φ_f = 0.546), Rhodamine 6G in EtOH (Φ_f = 0.94), or Cresyl Violet in MeOH (Φ_f = 0.54) as standards. Fluorescence decays were measured in a time-correlated single-photon counting (TCSPC) configuration under excitation by selected nanoLEDs (370, 455, or 570 nm). The instrument response was determined by measuring the light scattered by a Ludox suspension. The lifetimes were obtained from a re-convolution fit analysis of the decay profiles; the quality of the fits was judged by the reduced χ^2 value (χ^2 < 1.1). The reported lifetimes are within ±0.1 ns.

Two-Photon Absorption: TPA cross-sections (σ_2) were determined from the two-photon excited fluorescence (TPEF) cross-sections ($\sigma_2\Phi_f$) and the fluorescence emission quantum yields (Φ_f). The TPEF cross-sections of 10^{-4} M chloroform solutions were measured relative to fluorescein in 0.01 M aqueous NaOH in the range 715–980 nm using the well-established method described by Xu and Webb[28a] and the appropriate solvent-related refractive index corrections.[31] The quadratic dependence of the fluorescence intensity on the excitation power was checked for each sample and all wavelengths to verify that the measurements were carried out in intensity regimes in which saturation or photodegradation did not occur. Measurements were conducted using excitation sources delivering fs pulses. This was preferred to avoid excited-state absorption during the pulse duration, a phenomenon that has been shown to lead to overestimated TPA cross-sections. To span the 700–980 nm range, an Nd:YLF-pumped Ti:sapphire oscillator was used that generated 150 fs pulses at a frequency of 76 MHz. To span the 1000–1400 nm range, an Optical Parametric Oscillator (OPO) was added to the setup to collect and modulate the output signal of the Ti:sapphire oscillator. The excitation source was focused on the cuvette through a microscope objective (10 ×, NA 0.25). The fluorescence was detected in epifluorescence mode by means of a dichroic mirror (Chroma 675dcxru) and a barrier filter (Chroma e650sp-2p) by using a compact CCD spectrometer module BWTek BTC112E. Total fluorescence intensities were obtained by integrating the corrected emission. The experimental uncertainty of the action cross-sections determined by this method was estimated to be ±10 %.

Acknowledgments

M. M. M. R. thanks the Fundação para a Ciência e Tecnologia (Portugal) for financial support to the Portuguese NMR network (PT NMR Bruker Avance III 400-Univ. Minho) and European Fund for Regional Development (FEDER) – COMPETEQREN-EU for financial support to the research centre CQ/UM [PEst-C/QUI/UI0686/2013 (FCOMP-01-0124-FEDER-037302)] and a Ph. D. grant to M. C. R. C. (SFRH/BD/78037/2011). M. B.-D. acknowledges financial support from the Conseil Régional d'Aquitaine (Chair of Excellence to M. B.-D. and fellowship to V. H.). This study was carried out with financial support from the French State, managed by the French National Research Agency (ANR) within the framework of "the Investments for the future" Programme IdEx Bordeaux – LAPHIA (ANR-10-IDEX-03-02).

Keywords: Aldehydes · Cross-coupling · Donor–acceptor systems · Sulfur heterocycles · Fluorescence · Two-photon absorption

[1] M. Pawlicki, H. A. Collins, R. G. Denning, H. L. Anderson, *Angew. Chem. Int. Ed.* **2009**, *48*, 3244–3266; *Angew. Chem.* **2009**, *121*, 3292; F. Terenziani, C. Katan, E. Badaeva, E. Tretiak, M. Blanchard-Desce, *Adv. Mater.* **2008**, *20*, 4641–4678; G. S. He, L.-S. Tan, Q. Zheng, P. N. Prasad, *Chem. Rev.* **2008**, *108*, 1245–1330.
[2] H. M. Kim, B. R. Cho, *Chem. Commun.* **2009**, 153–164.
[3] D. Kim, H. G. Ryu, K. H. Ahn, *Org. Biomol. Chem.* **2014**, *12*, 4550–4566.
[4] A. S. Dvornikov, E. P. Walker, P. M. Rentzepis, *J. Phys. Chem. A* **2009**, *113*, 13633–13644; C. C. Corredor, Z.-L. Huang, K. D. Belfield, A. R. Morales, M. V. Bondar, *Chem. Mater.* **2007**, *19*, 5165–5173.
[5] S. Kawata, H.-B. Sun, T. Tanaka, K. Takada, *Nature* **2001**, *412*, 697–698; I. Sakellari, E. Kabouraki, D. Gray, V. Purlys, C. Fotakis, A. Pikulin, N. Bityurin, M. Vamvakaki, M. Farsari, *ACS Nano* **2012**, *6*, 2302–2311.
[6] Q. Zheng, G. S. He, P. N. Prasad, *Chem. Phys. Lett.* **2009**, *475*, 250–255.
[7] a) W. Denk, J. H. Strickler, W. W. Webb, *Science* **1990**, *248*, 73–76; b) K. Svoboda, W. Denk, D. Kleinfeld, D. W. Tank, *Nature* **1997**, *385*, 161–165; M. Blanchard-Desce, *C. R. Phys.* **2002**, *3*, 439–448; H. M. Kim, B. R. Cho, *Chem. Asian J.* **2011**, *6*, 58–69.
[8] K. Ogawa, Y. Kobuke, *Org. Biomol. Chem.* **2009**, *7*, 2241–2246; J. R. Starkey, A. K. Rebane, M. A. Drobizhev, F. Meng, A. Gong, A. Elliott, K. McInnerney, C. W. Spangler, *Clin. Cancer Res.* **2008**, *14*, 6564–6573; H. A. Collins, M. Khurana, E. H. Moriyama, A. Mariampillai, E. Dahlstedt, M. Balaz, M. K. Kuimova, M. Drobizhev, V. X. D. Yang, D. Phillips, A. Rebane, B. C. Wilson, H. L. Anderson, *Nat. Photonics* **2008**, *2*, 420–424.
[9] M. Albota, D. Beljonne, J. L. Bredas, J. E. Ehrlich, J. Y. Fu, A. A. Heikal, S. E. Hess, T. Kogej, M. D. Levin, S. R. Marder, D. McCord-Maughon, J. W. Perry, H. Rockel, M. Rumi, C. Subramaniam, W. W. Webb, X. L. Wu, C. Xu, *Science* **1998**, *281*, 1653–1656.
[10] a) V. Parthasarathy, S. Fery-Forgues, E. Campioli, G. Recher, F. Terenziani, M. Blanchard-Desce, *Small* **2011**, *7*, 3219–3229; b) L. Zou, Y. Liu, N. Ma, E. Maçôas, J. M. G. Martinho, M. Pettersson, X. Chen, J. Qin, *Phys. Chem. Chem. Phys.* **2011**, *13*, 8838–8846; c) M. Zhang, M. Li, F. Li, D. Zhang, J. Zhang, F. Yi, C. Huang, *Tetrahedron Lett.* **2007**, *48*, 2329–2333; d) Q. Li, J. Huang, A. Zhong, C. Zhong, M. Peng, J. Liu, Z. Pei, Z. Huang, J. Qin, Z. J. Li, *J. Phys. Chem. B* **2011**, *115*, 4279–4285; e) V. Hrobáriková, P. Hrobárik, P. Gajdoš, I. Fitilis, M. Fakis, P. Persephonis, P. Zahradník, *J. Org. Chem.* **2010**, *75*, 3053–3068; f) H. Zhou, F. Zhou, S. Tang, P. Wu, Y. Chen, Y. Tu, J. Wu, Y. Tian, *Dyes Pigm.* **2012**, *92*, 633–641; g) P. Lind, M. Carlsson, B. Eliasson, E. Glimsdal, M. Lindgren, C. Lopes, L. Boman, P. Norman, *Mol. Phys.* **2009**, *107*, 629–641; h) P. Hrobárik, V. Hrobáriková, I. Sigmundová, P. Zahradník, M. Fakis, I. Polyzos, P. Persephonis, *J. Org. Chem.* **2011**, *76*, 8726–8736; i) Y. M. Poronik, V. Hugues, M. Blanchard-Desce, D. T. Gryko, *Chem. Eur. J.* **2012**, *18*, 9258–9266; j) G. Argouarch, R. Veillard, T. Roisnel, A. Amar, H. Meghezzi, A. Boucekkine, V. Hugues, O. Mongin, M. Blanchard-Desce, F. Paul, *Chem. Eur. J.* **2012**, *18*, 11811–11827; k) K. Amro, J. Daniel, G. Clermont, T. Bsaibess, M. Pucheault, E. Genin, M. Vaultier, M. Blanchard-Desce, *Tetrahedron* **2014**, *70*, 1903–1909; l) A. I. Ciuciu, D. Firmansyah, V. Hugues, M. Blanchard-Desce, D. T. Gryko, L. Flamigni, *J. Mater. Chem. C* **2014**, *2*, 4552–4565; m) M. Grzybowski, V. Hugues, M. Blanchard-Desce, D. T. Gryko, *Chem. Eur. J.* **2014**, *20*, 12493–12501; n) P. Hrobárik, V. Hrobáriková, V. Semak, P. Kasák, E. Rakovský, I. Polyzos, M. Fakis, P. Persephonis, *Org. Lett.* **2014**, *16*, 6358–6361; o) M. Grzybowski, E. Glod-

kowska-Mrowka, V. Hugues, M. Blanchard-Desce, D. T. Gryko, *Chem. Eur. J.* **2015**, *21*, 9101–9110; p) R. Orłowski, M. Banasiewicz, G. Clermont, F. Castet, R. Nazir, M. Blanchard-Desce, D. T. Gryko, *Phys. Chem. Chem. Phys.* **2015**, *17*, 23724–23731.

[11] a) V. P. Rao, K. Y. Wong, A. K.-Y. Jean, K. J. Drost, *Chem. Mater.* **1994**, *6*, 2210–2212; b) M. Blenkle, P. Boldt, C. Bräuchle, W. Grahn, I. Ledoux, H. Nerenz, S. Stadler, J. Wichern, J. Zyss, *J. Chem. Soc. Perkin Trans. 2* **1996**, 1377–1384; c) P. Boldt, G. Bourhill, C. Bräuchle, Y. Jim, R. Kammler, C. Müller, J. Rase, J. Wichern, *Chem. Commun.* **1996**, 793–795; d) I. Cazenobe, I. Ledoux, J. Zyss, P. Boldt, J. Wichern, T. H. Kirchberger, J. Rase, *Opt. Mater.* **1998**, *9*, 280–285; e) A. B. Marco, R. Andreu, S. Franco, J. Garín, J. Orduna, B. Villacampa, R. Alicante, *Tetrahedron* **2013**, *69*, 3919–3926; f) A. B. Marco, R. Andreu, S. Franco, J. Garín, J. Orduna, B. Villacampa, B. E. Diosdado, J. L. Navarrete, J. Casado, *Org. Biomol. Chem.* **2013**, *11*, 6338–6349.

[12] a) O.-K. Kim, A. Fort, M. Barzoukas, M. Blanchard-Desce, J.-M. Lehn, *J. Mater. Chem.* **1999**, *9*, 2227–2232; b) P. J. Skabara in *Handbook of Thiophene-based Materials*, vol. 1 (Eds.: I. F. Perepichka, D. F. Perepichka), Wiley, Chichester, **2009**, chapter 3.

[13] For reviews, see: a) V. P. Litvinov, Y. A. L. Gol'dfarb, *Adv. Heterocycl. Chem.* **1976**, *19*, 123–214; b) A. Comel, G. Sommen, G. Kirsch, *Mini-Rev. Org. Chem.* **2004**, *1*, 367–374; c) V. P. Litvinov, *Russ. Chem. Rev.* **2005**, *74*, 217–248; d) V. P. Litvinov, *Adv. Heterocycl. Chem.* **2006**, *90*, 125–203; e) M. E. Cinar, T. Ozturk, *Chem. Rev.* **2015**, *115*, 3036–3140.

[14] For some selected examples, see: a) J. Zhang, H.-B. Li, S.-L. Sun, Y. Geng, Y. Wu, Z.-M. Su, *J. Mater. Chem.* **2012**, *22*, 568–576; b) B.-G. Kim, C.-G. Zhen, E. J. Jeong, J. Kieffer, J. Kim, *Adv. Funct. Mater.* **2012**, *22*, 1606–1612; c) X. Zong, M. Liang, T. Chen, J. Jia, L. Wang, Z. Sun, S. Xue, *Chem. Commun.* **2012**, *48*, 6645–6647; d) H. Choi, I. Raabe, D. Kim, F. Teocoli, C. Kim, K. Song, J.-H. Yum, J. Ko, M. K. Nazeeruddin, M. Gratzel, *Chem. Eur. J.* **2010**, *16*, 1193–1201; e) G. Zhang, Y. Bai, R. Li, D. Shi, S. Wenger, S. M. Zakeeruddin, M. Grätzel, P. Wang, *Energy Environ. Sci.* **2009**, *2*, 92–95; f) D. Kim, C. Kim, H. Choi, K. Song, M.-S. Kang, J. Ko, *J. Photochem. Photobiol. A* **2011**, *219*, 122–131; g) M. Xu, R. Li, N. Pootrakulchote, D. Shi, J. Guo, Z. Yi, S. M. Zakeeruddin, M. Grätzel, P. Wang, *J. Phys. Chem. C* **2008**, *112*, 19770–19776; h) H.-G. Bae, C.-C Lee, J.-B. Kim, H.-D. Moon, T.-J. Park, J.-H. Baek, H.-T. Yang, H.-C. An, *PCT Int. Appl.* WO 2009051390 A2 20090423, **2009**; i) A. Mishra, M. K. R. Fischer, P. Bäuerle, *Angew. Chem. Int. Ed.* **2009**, *48*, 2474–2499; *Angew. Chem.* **2009**, *121*, 2510.

[15] a) J. I. Tietz, J. R. Mastriana, P. Sampson, A. J. Seed, *Liq. Cryst.* **2012**, *39*, 515–530; b) R. M. Gipson, P. Sampson, A. J. Seed, *Liq. Cryst.* **2010**, *37*, 101–108.

[16] M. C. G. M. Heeney, W. Zhang, K. S. Whitehead, D. D. C. Bradley, I. McCullochd, A. J. Campbell, *Chem. Commun.* **2008**, 1079–1081.

[17] a) C. B. Nielsen, I. McCulloch, *Prog. Polym. Sci.* **2013**, *38*, 2053–2069; b) A. Capan, H. Veisi, A. C. Goren, T. Ozturk, *Macromolecules* **2012**, *45*, 8228–8236; c) N. Hergué, P. Frère, J. Roncali, *Org. Biomol. Chem.* **2011**, *9*, 588–595; d) K. Nakayama, Y. Hirose, J. Soeda, M. Yoshizumi, T. Uemura, M. Uno, W. Li, M. J. Kang, M. Yamagishi, Y. Okada, E. Miyazaki, Y. Nakazawa, A. Nakao, K. Takimiya, J. Takeya, *Adv. Mater.* **2011**, *23*, 1626–1629; e) K. Niimi, S. Shinamura, I. Osaka, E. Miyazaki, K. Takimiya, *J. Am. Chem. Soc.* **2011**, *133*, 8732–8739.

[18] a) M. M. M. Raposo, G. Kirsch, *Tetrahedron* **2003**, *59*, 4891–4899; b) M. M. M. Raposo, A. M. C. Fonseca, G. Kirsch, *Tetrahedron* **2004**, *60*, 4071–4078; c) S. P. G. Costa, R. M. F. Batista, P. Cardoso, M. Belsey, M. M. M. Raposo, *Eur. J. Org. Chem.* **2006**, 3938–3946; d) M. M. M. Raposo, A. M. R. C. Sousa, A. M. C. Fonseca, G. Kirsch, *Tetrahedron* **2006**, *62*, 3493–3501; e) C. Herbivo, A. Comel, G. Kirsch, M. M. M. Raposo, *Tetrahedron* **2009**, *65*, 2079–2086; f) M. C. R. Castro, M. Belsley, A. M. C. Fonseca, M. M. M. Raposo, *Tetrahedron* **2012**, *68*, 8147–8155.

[19] a) M. M. M. Raposo, A. M. R. C. Sousa, G. Kirsch, P. Cardoso, M. Belsey, E. M. Gomes, A. M. C. Fonseca, *Org. Lett.* **2006**, *8*, 3681–3684; b) A. Wojciechowski, M. M. M. Raposo, M. C. R. Castro, W. Kuznik, I. Fuks-Janczrek, F. Bureš, I. V. Kityk, *J. Mater. Sci. Mater. Electron.* **2014**, *25*, 1745–1750.

[20] a) C. Herbivo, A. Comel, G. Kirsch, A. M. C. Fonseca, M. Belsley, M. M. M. Raposo, *Dyes Pigm.* **2010**, *86*, 217–226; b) E. Genin, V. Hugues, G. Clermont, C. Herbivo, A. Comel, M. C. R. Castro, M. M. M. Raposo, M. Blanchard-Desce, *Photochem. Photobiol. Sci.* **2012**, *11*, 1756–1766.

[21] a) M. Blanchard-Desce, V. Alain, P. V. Bedworth, S. R. Marder, A. Fort, C. Runser, M. Barzoukas, S. Lebus, R. Wortmann, *Chem. Eur. J.* **1997**, *3*, 1091–1104; b) V. Alain, L. Thouin, M. Blanchard-Desce, U. Gubler, C. Bosshard, P. Günter, J. Muller, A. Fort, M. Barzoukas, *Adv. Mater.* **1999**, *11*, 1210–1214.

[22] M. Kuhn, F. C. Falk, J. Paradies, *Org. Lett.* **2011**, *13*, 4100–4103.

[23] D. Prim, G. Kirsch, *J. Chem. Soc. Perkin Trans. 1* **1994**, 2603–2606.

[24] L. S. Fuller, B. Iddon, K. A. Smith, *J. Chem. Soc. Perkin Trans. 1* **1997**, 3465–3470.

[25] J. D. Prugh, G. D. Hartman, P. J. Mallorga, B. M. McKeever, S. R. Michelson, M. A. Murcko, H. Schwam, R. L. Smith, J. M. Sondey, *J. Med. Chem.* **1991**, *34*, 1805–1818.

[26] S. Cai, G. Tian, X. Li, J. Su, H. Tian, *J. Mater. Chem. A* **2013**, *1*, 11295–11305.

[27] F. Quist, C. M. L. Van de Velve, D. Didier, A. Teshome, K. Clays, S. Sergeyev, *Dyes Pigm.* **2009**, *81*, 203–210.

[28] a) C. Xu, W. W. Webb, *J. Opt. Soc. Am. B* **1996**, *13*, 481–491; b) M. A. Albota, C. Xu, W. W. Webb, *Appl. Opt.* **1998**, *37*, 7352–7356.

[29] M. Barzoukas, M. Blanchard-Desce, *J. Chem. Phys.* **2000**, *113*, 3951–3959.

[30] a) D. F. Eaton, *Pure Appl. Chem.* **1988**, *60*, 1107–1114; b) G. A. Crosby, J. N. Demas, *J. Phys. Chem.* **1971**, *75*, 991–1024.

[31] M. H. V. Werts, N. Nerambourg, D. Pelegry, Y. L. Grand, M. Blanchard-Desce, *Photochem. Photobiol. Sci.* **2005**, *4*, 531–538.

Received: July 1, 2016
Published Online: October 6, 2016

